Climate Dynamics (1997) 13: 349–358

Climate
Dynamics

Sensitivity of a global ice–ocean model to the Bering Strait throughflow

H. Goosse, J. M. Campin, T. Fichefet, E. Deleersnijder

Institut d'Astronomie et de Géophysique Georges Lemaître, Université Catholique de Louvain, 2 Chemin du Cyclotron, B-1348 Louvain-la-Neuve, Belgium

Received: 27 October 1995/Accepted: 20 November 1996

Abstract. To understand the influence of the Bering Strait on the World Ocean's circulation, a model sensitivity analysis is conducted. The numerical experiments are carried out with a global, coupled ice–ocean model. The water transport through the Bering Strait is parametrized according to the geostrophic control theory. The model is driven by surface fluxes derived from bulk formulae assuming a prescribed atmospheric seasonal cycle. In addition, a weak restoring to observed surface salinities is applied to compensate for the global imbalance of the imposed surface freshwater fluxes. The freshwater flux from the North Pacific to the North Atlantic associated with the Bering Strait throughflow seems to be an important element in the freshwater budget of the Greenland and Norwegian seas and of the Atlantic. This flux induces a freshening of the North Atlantic surface waters, which reduces the convective activity and leads to a noticeable (6%) weakening of the thermohaline conveyor belt. It is argued that the contrasting results obtained by Reason and Power are due to the type of surface boundary conditions they used.

1 Introduction

Relatively fresh surface waters (with a salinity of about 32.5 psu) are carried from the North Pacific to the Arctic through the Bering Strait at a rate of about 1 Sv (Coachman and Aagaard 1988; Roach et al. 1995) (1 Sv = 10^6 m^3 s^{-1}). This northward flow is important because of its influence on the regional physical oceanography (e.g., Muench et al. 1988) and the high biological productivity it sustains over the Bering Shelf (e.g., Walsh et al. 1989). The Bering Strait also plays a role in global-scale processes. In particular, it contributes to the global freshwater budget by balancing partly the atmospheric transport of freshwater from the Atlantic to the Pacific (Broecker et al. 1990; Wijfels et al. 1992).

The freshwater deficit of the Atlantic is compensated by the "conveyor belt" since it carries southward deep, salty water, termed North Atlantic Deep Water (NADW), the southward flow being balanced by fresh waters originating mainly from the South Atlantic and, of lesser magnitude, from the Arctic (Broecker 1991). The exchanges between the Arctic and the North Atlantic are obviously influenced by the northward flow through the Bering Strait, suggesting that the latter may control, to a certain extent, the global thermohaline circulation and, consequently, the global climate.

Using a two-box model, Shaffer and Bendtsen (1994) showed that increasing the water flow through the Bering Strait from 0 to 1 Sv reduced the intensity of the North Atlantic thermohaline circulation by 20%. This was explained as follows: the freshwater transport through the Bering Strait tends to decrease the salinity of the North Atlantic surface waters, which reduces convective activity, deep-water formation, and thus the southward flux of NADW. A further increase of the Bering Strait throughflow to 1.1 Sv completely stopped deep-water formation in the North Atlantic. Accordingly, Shaffer and Bendtsen (1994) suggested that the North Atlantic deep-water production is more sensitive to perturbations when the flow through the Bering Strait is large. They further hypothesized that the enhanced climate variability during the last interglacial period may be due to higher sea level enabling a significant flow through the Bering Strait.

The results of Reason and Power (1994) are in marked contrast to those of Shaffer and Bendtsen (1994). They conducted a sensitivity study by means of an ocean circulation model (OGCM): in the first experiment, the Bering Strait was closed, whereas, in the second one, the strait was open. Under strong restoring surface boundary conditions, they found that the strength of the NADW overturning cell increased by about 8% when opening the

Correspondence to: H. Goosse

This paper was presented at the Third International Conference on Modelling of Global Climate Change and Variability, held in Hamburg 4–8 Sept. 1995 under the auspices of the Max Planck Institute for Meteorology, Hamburg. Editor for these papers is L. Dümenil.

Bering Strait. Under mixed boundary conditions (i.e., with a restoring condition for the surface temperature and a prescribed surface salt flux derived from the restoring run), virtually no difference was found between the experiments with the Bering Strait open or closed. However, a different interpretation of their results could be obtained from the figures displayed in their paper (Rahmstorf, personal communication 1996). In fact, the opening of the Bering Strait simply yields an additional southward flux on the circulation existing in the Atlantic when the Bering Strait was closed. This flux is almost barotropic with restoring boundary conditions (their Fig. 1c) and confined to the top 1500 m with mixed boundary conditions (their Fig. 5c). In the two cases, the opening of the Bering Strait appears to have a very small effect on the overturning circulation in the Atlantic and on the NADW formation.

Under restoring boundary conditions, the difference in the surface freshwater fluxes between experiments with and without a Bering Strait may be of the same order of magnitude as the fluxes induced by the opening of the Bering Strait. The same problem can occur under mixed boundary conditions since the two salt fluxes used by Reason and Power (1994) are diagnosed from the two corresponding experiments under restoring boundary conditions. These flux differences may compensate for the effects of the Bering Strait throughflow and, thus, may mask the influence of the Bering Strait on the ocean general circulation. This stresses the crucial importance of the surface boundary conditions for examining the role of the Bering Strait in the global ocean circulation.

In this study, we perform a sensitivity study bearing some similarity to that of Reason and Power (1994). However, in our simulations, sea ice is explicitly modelled and the surface boundary conditions are believed to be more appropriate (see Sect. 4). As will be seen, our results are qualitatively consistent with those of Shaffer and Bendtsen (1994).

2 Description of the model

The model used here results from the coupling of a global, free-surface OGCM (Deleersnijder and Campin 1995) with a comprehensive sea–ice model (Fichefet and Morales Maqueda 1996, Sensitivity of a global sea ice model to the treatment of ice thermodynamics and dynamics, submitted to Journal of Geophysical Research). The OGCM is a primitive-equation model resting on the usual set of assumptions, i.e., the hydrostatic equilibrium and the Boussinesq approximation (e.g., Bryan 1969). In the horizontal plane, spherical coordinates are used, while the "z-coordinate" underlies the vertical discretization. The sea–ice model has representations of both thermodynamic and dynamic processes. A 3-layer model (Fichefet and Gaspar 1988) simulates the changes of snow and ice thicknesses and heat contents in response to the surface and bottom heat fluxes. The variations of ice compactness due to thermal processes are determined following the approach proposed by Häkkinen and Mellor (1990). The ice model also incorporates a parametrization of the latent heat storage in brine pockets and a simple scheme for snow–ice formation. For ice dynamics computation, sea–ice is considered to behave as a two-dimensional viscous-plastic continuum (Hibler 1979). The oceanic heat flux at the base of the ice slab is calculated by imposing a thermodynamic equilibrium between ice and the water underneath. Both the temperature at the base of the ice and the temperature of the top oceanic layer are supposed to be equal to the freezing point of seawater. To maintain this equilibrium, the oceanic heat flux must compensate exactly for the net heat gain of the first oceanic layer (Fichefet and Gaspar 1988). The water stress on ice is taken to be a quadratic function of the relative velocity between ice and the top layer of the ocean, using a drag coefficient $c_w = 5 \times 10^{-3}$.

The governing equations of the model are solved numerically by using a finite-volume technique on an Arakawa B-grid. The horizontal resolution is $3^\circ \times 3^\circ$. Vertically, there are 20 levels ranging in thickness from 10 m at the surface to 750 m in the deep ocean. A realistic bathymetry is used. The global grid is obtained by patching together two spherical grids. The first one is a standard spherical grid covering the whole World Ocean, except for the northern Atlantic and the Arctic, which are represented on a spherical grid having its poles on the equator, in order to avoid the North Pole singularity. The two grids are connected in the equatorial Atlantic (Deleersnijder et al. 1993; Eby and Holloway 1994; Coward et al. 1994). The horizontal eddy diffusivity and viscosity of the ocean model are set equal to $150\,m^2\,s^{-1}$ and $10^5\,m^2\,s^{-1}$, respectively. Vertical mixing is prescribed following Pacanowski and Philander (1981).

The model is driven by surface fluxes of heat, freshwater, and momentum determined from the empirical bulk formulae described in Oberhuber (1988). Input fields consists of monthly climatological surface air temperatures and dew points (Crutcher and Meserve 1970; Taljaard et al. 1969), surface winds and wind stresses (Trenberth et al. 1989), cloud fractions (Berliand and Strokina 1980), and precipitation rates (Jaeger 1976). The fraction of precipitation falling as snow is derived from the surface air temperature as in Ledley (1985). The river runoff is taken from the annual mean climatology of Baumgartner and Reichel (1975). Owing to inaccuracies in the precipitation and runoff data and in the evaporation computed by the model, the net freshwater flux at the surface exhibits a slight imbalance inducing a drift in the simulated global salinity. To remedy this problem, a relaxation to annual mean observed salinities (Levitus 1982) is applied in the surface layer with a time constant of two months. Note that there is no restoring over salinity on the continental shelves of the Bering and Chukchi seas, located on both sides of the Bering Strait.

3 Parametrization of the water and ice transports through the Bering Strait

The width of the Bering Strait is about 85 km, which is generally smaller than the grid size of a coarse-resolution OGCM. Therefore, if the flow from the Pacific to the Arctic was to be calculated explicitly in the model, it would be necessary to artificially widen the Bering Strait. In particular, if a B-grid is used, as in our model, the width

of the model strait must be at least equal to two horizontal space increments. In our case, this would lead to a numerical width about seven times larger than the exact one, which may not be the best possible modelling option. Our grid system presents an additional difficulty: the coordinate systems on both sides of the Bering Strait do not match each other (Deleersnijder et al. 1993). To avoid these technical problems, we parametrize the water and sea–ice flows through the Bering Strait, rather than try to represent them explicitly by means of finite-difference approximations equivalent to those used at every other location. In other words, the Bering Strait is simulated by removing water and sea ice at an appropriate rate from the vicinity of the strait on the Pacific side, and pouring it into the Arctic Ocean, close to the strait.

The mean northward water flow through the Bering Strait is believed to be driven by the difference in sea-surface elevation between the North Pacific and the Arctic oceans, the Pacific being higher. This sea-level slope results from the density difference between the two basins (Stigebrandt 1984; Overland and Roach 1987). According to in situ measurements (Nihoul et al. 1993; Roach et al. 1995) and regional-scale modelling (Deleersnijder 1994), the horizontal velocity exhibits small vertical variations in the vicinity of the Bering Strait.

As shown in the numerical study of Overland and Roach (1987), the northward flow may be assumed to obey the geostrophic control theory (e.g., Toulany and Garret 1984). Under this hypothesis, cross-strait geostrophic equilibrium holds true (roughly east–west). It follows that the flow through the strait is related to the cross-strait surface elevation difference, which must be smaller than the sea-level difference between the Pacific and Arctic basins. Then, assuming weak friction and low frequency motion, the maximum water flow through the strait is given by

$$Q_{max} = \frac{gh}{f}(\eta_{Pac} - \eta_{Arc}) \tag{1}$$

where g, f and h represent the gravitational acceleration ($=9.8\,\mathrm{m\,s^{-2}}$), the Coriolis parameter ($\approx 1.4\times10^{-4}\,\mathrm{s^{-1}}$) and the sea depth ($\approx 50$ m), respectively; η_{Pac} denotes the sea-surface elevation on the Pacific side of the Bering Shelf, while η_{Arc} is the elevation on the Arctic side. The actual flow through the strait is taken to be $Q = \alpha Q_{max}$, where α is a dimensionless coefficient smaller than unity. After appropriate tuning, we set $\alpha = 0.5$. It must be stressed that the rationale leading to out parametrization of Q rests on the assumption that the flow is barotropic. If we were to take into account a significant baroclinic component, it would prove much more difficult to derive a relevant parametrization. The northward water flow is used to calculate the corresponding transport of heat and salt.

Sea–ice flow through the Bering Strait is also parametrized. An estimate of the northward ice velocity, v_{ice}, is derived from the momentum equation by assuming pure shearing in an infinite channel (e.g., Hibler 1986):

$$v_{ice} = v_w + sign(F)\sqrt{\frac{|F|}{\rho_w c_w}} \tag{2}$$

with

$$F = \tau_a - mg\frac{\partial\eta}{\partial x} - \frac{2P'}{W}sign(v_{ice})$$

where v_w, τ_a, and P' denote, respectively, the northward water velocity, the northward component of the air–ice stress, and the resistance to shearing, computed after Hibler (1979); W, the width of the strait, is taken to be 85 km; finally, ρ_w represents the seawater density.

4 Results and discussion

Two numerical experiments are carried out with the model: one with the Bering Strait open (hereafter OP), the other with the strait closed (hereafter CL). For both model runs, the initial conditions are an equlibrium state obtained under robust-diagnostic forcing. The results are analyzed after 300 years of integration, when the salinity and temperature fields evolve quite slowly. It is clear that this rather short integration length, which is dictated by the computing cost of the model, is not sufficient to reach a full equilibrium state. Important transitions in ocean circulation may occur after more than 300 years even if the temperature and salinity drifts are very slow (e.g., Rahmstorf 1995). Caution must therefore be exercised when drawing conclusions from the experiments presented here. Nevertheless, it should be noted that no transition or inversion in the trend of model evolution has been noticed during the two experiments. Furthermore, the experiment OP has been prolonged for 200 years and the results were nearly identical to those discussed here.

In OP, the annual mean of the transport Q is 1.15 Sv, which is somewhat larger than the estimated 0.8 Sv of Coachman and Aagaard (1988) and Roach et al. (1995). The seasonal cycle, which is mainly due to the variations in the wind stress, exhibits an amplitude (half the maximum minus minimum) of about 0.2 Sv. The maximum transport occurs in summer. The phase of the simulated cycle is in agreement with the observations of Coachman and Aagaard (1988) and Roach et al. (1995), but the amplitude appears underestimated by roughly a factor of 1.5. There is no reliable measurement of the annual mean ice flow through the Bering Strait. It seems however certain that this transport is small (Pease and Salo 1987; Simonsen and Haugan 1996), which is in accordance with our numerical estimate being as small as 2.9×10^{-3} Sv (southwards).

Opening the Bering Strait modifies the barotropic stream function by a few Sverdrups, as depicted in Fig. 1. The return flow towards the Atlantic Ocean through the Indonesian seas and along the eastern coast of Africa is slightly reduced, while the northward flow in the western Pacific is enhanced. In the Atlantic, the Gulf Stream intensity diminishes, as well as the strength of the subarctic gyre. As a consequence of the latter reduction, there is less Atlantic water entering the Norwegian Sea and a smaller export of Greenland Sea and Iceland Sea waters through the Denmark Strait (between Iceland and Greenland).

Some changes in the path of the Antartic Circumpolar Current are also observed, while the magnitude of the

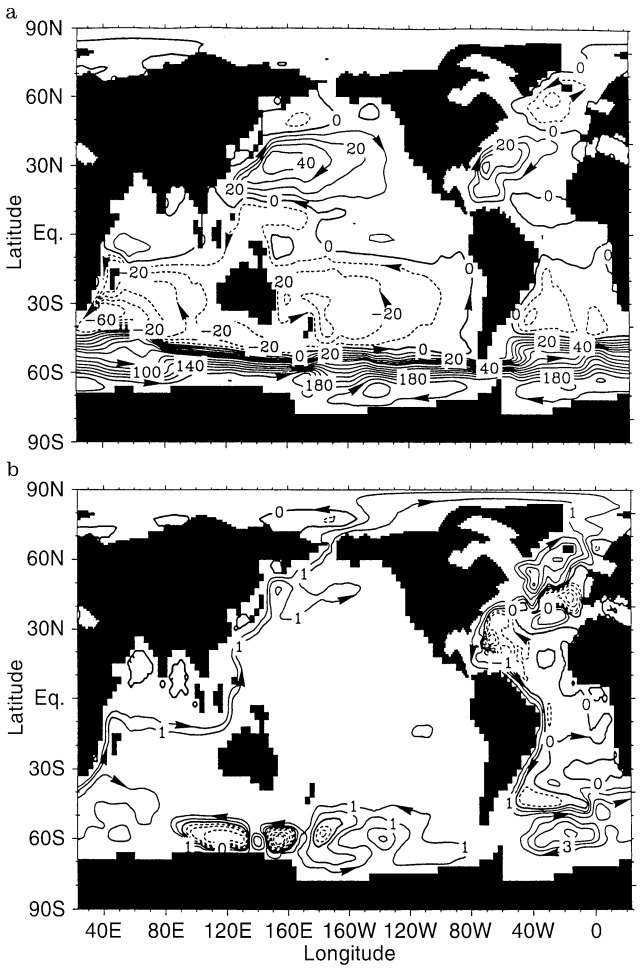

Fig. 1a,b. Annual mean barotropic streamfunction. **a** Experiment OP; contour interval is 10 Sv between − 60 Sv and + 60 Sv and 20 Sv otherwise; **b** OP minus CL; contour interval is 0.5 Sv between − 1 Sv and + 1 Sv and 1 Sv otherwise

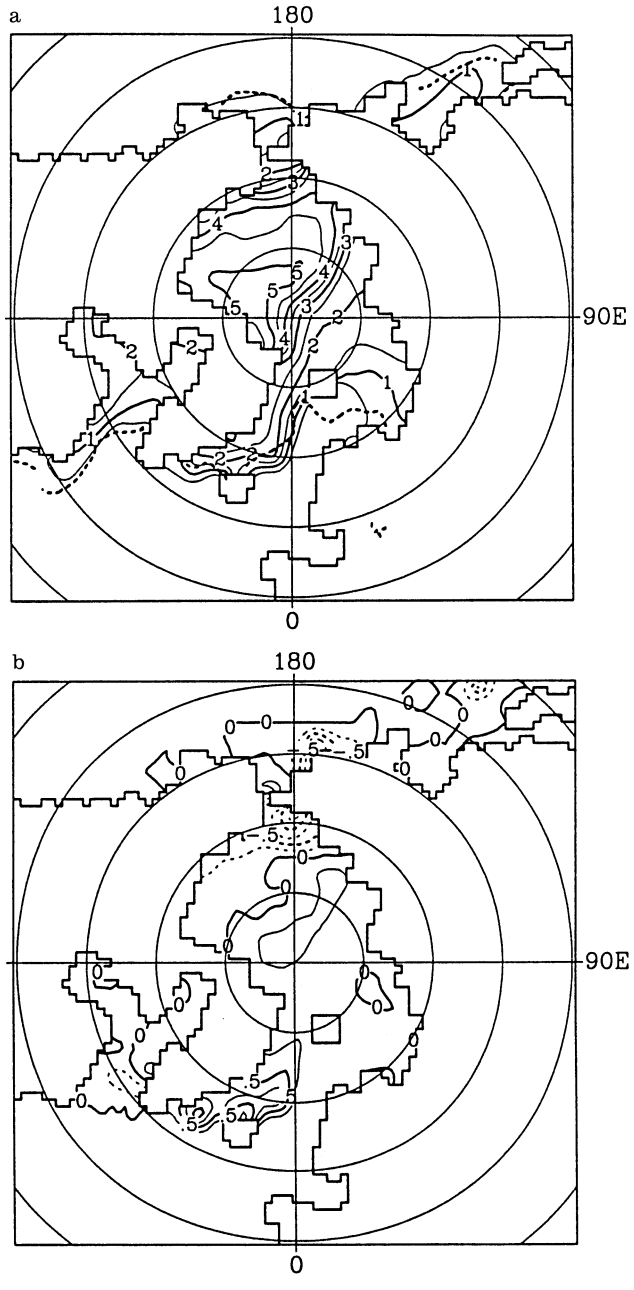

Fig. 2a, b. Ice thickness (in metres) for March in the Arctic. **a** Experiment OP; contour interval is 0.5 m. The *dashed line* represents the observed ice edge in March (Gloersen et al. 1992), defined as the 15% ice concentration. **b** OP minus CL; contour interval is 0.25 m

transport through the Drake Passage is nearly the same in the two experiments. These modifications seem to be related to the internal variability of this strong current.

The water flow through the Bering Strait is approximately balanced by an increase in the Farm Strait, between Greenland and Spitzbergen, outflow. Opening the Bering Strait raises the southward water transport through Fram Strait from 2.70 Sv to 3.77 Sv, i.e., a difference of 1.07 Sv which is almost equivalent to the 1.15 Sv crossing the Bering Strait. Enhancing the water transport increases, by dynamical coupling, the southward ice flow through Fram Strait from 6.8×10^4 to 7.7×10^4 m^3 of ice per second.

In CL, the ice edge is generally too far southwards in the North Pacific. In OP, there is an increased transport of relatively warm water towards the Bering Sea, enhancing the ice melting on both sides of the strait, so that the ice edge location is more realistically simulated. This is illustrated for March in Fig. 2. The seasonal cycle of the Arctic sea–ice extent is reasonably well simulated: the agreement between the model and observations (Gloersen et al. 1992) is quite good in winter (Fig. 2a) as well as in summer (not shown).

The oceanic region located off the southeastern coast of Greenland is an area of year-long ice melting, the ice coming from the north. Consequently, the stronger transport through Fram Strait in OP leads to an ice edge located further southwards along the Greenland coast and to higher ice thicknesses there (Fig. 2b). Furthermore, the ice melting in the Greenland and Norwegian seas is smaller in OP (2.9×10^4 m^3 s^{-1} in annual mean) than in CL (4.0×10^4 m^3 s^{-1} in annual mean). This reflects the oceanic heat flux at the ice base being weaker in OP. The additional amount of ice transported through Fram Strait

in OP does not melt in the Greenland and Norwegian seas, but is advected to the North Atlantic through the Denmark Strait.

Since the Bering Strait waters are saltier than the Arctic surface waters close to the Bering Strait, the salinity in the top layers of the Arctic ocean is larger in OP than in CL (Fig. 3a). On the other hand, the Arctic surface waters, as well as the North Pacific surface waters, are fresher than the North Atlantic surface waters. The opening of the Bering Strait induces a transport of freshwater from the North Pacific and the Arctic to the North Atlantic. Thus, the surface salinity in the GIN Sea (Greenland, Iceland and Norwegian seas, defined more precisely in the Appendix) is significantly smaller (Fig. 3a), particularly along the Greenland coast where the East Greenland current carries the relatively fresh Arctic waters southwards. Furthermore, there is an intense ice melting close to Iceland in OP (even if the ice melting averaged over the whole GIN Sea decreases in OP compared to CL). This leads to a particularly strong decrease in surface salinity there.

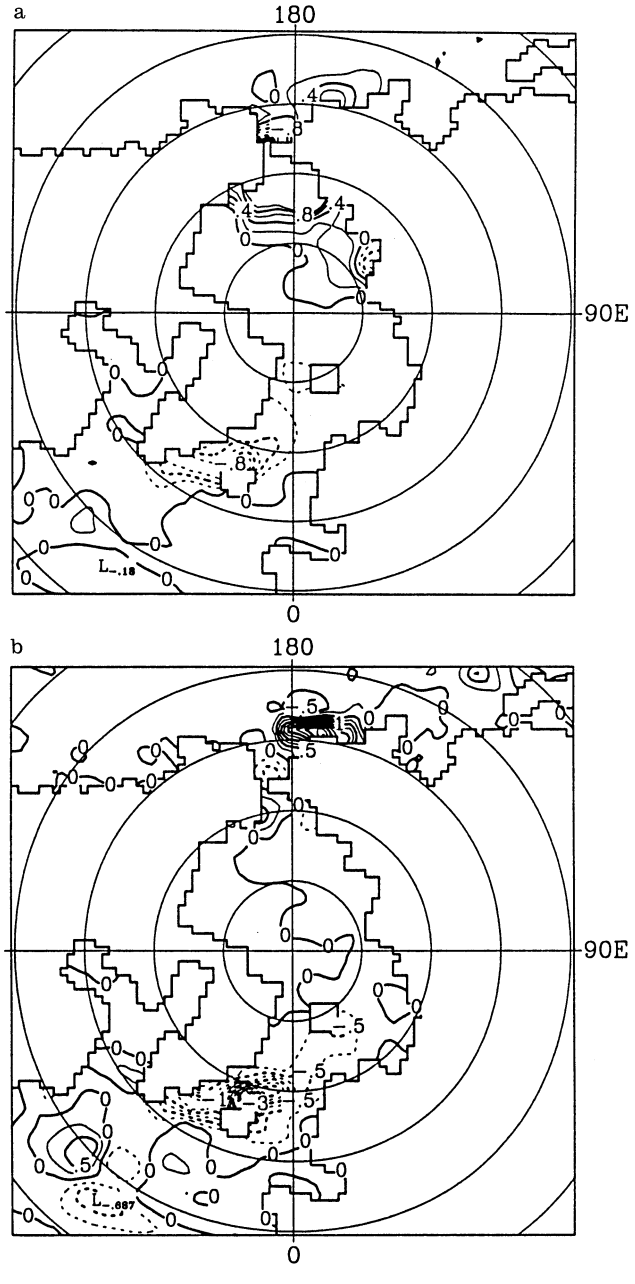

Fig. 3. **a** OP minus CL sea-surface salinity; contour interval is 0.2 psu. **b** OP minus CL sea-surface temperature; contour interval is 0.25 °C

The influence of cold Arctic water masses and sea–ice melting is also apparent in the sea-surface temperature distribution (Fig. 3b). In OP, there is a general cooling which is the most pronounced along the Greenland coast. The region located northwest of Iceland is ice-covered in OP but not in CL. In OP, the temperature of the top oceanic level remains at the freezing point during winter. Furthermore, the oceanic heat flux needed to melt ice limits the temperature increase in spring and summer. As a consequence the temperature decrease in this zone between CL and OP can reach 3 °C (Fig. 3b). These explanations are also valid for the area located southwest of Iceland, where the salinity and the temperature are much lower in OP than in CL (Fig. 3). The reduction of the inflow of salty and warm Atlantic waters in the GIN Sea can also play a minor role in the temperature and salinity decrease (see Appendix).

The surface temperature changes between the two experiments are less marked in the Arctic (Fig. 3b), since the temperature is close to freezing point during most of the year owing to the presence of sea ice. South of the Bering Strait, on the continental shelf, the small southward ice transport and the contact with Arctic waters generates an increase in the ice thickness and a decrease in both temperature and salinity. The eastern Bering Strait undergoes a noticeable increase in salinity and a significant warming in OP. This is because the Pacific waters on their way to the Bering Strait prevent ice formation in this region and trigger some convective events (caused by strong heat flux to the atmosphere), these events carrying heat and salt from the deep ocean to the surface.

In OP, convection decreases in a meridional band located in the centre of the GIN Sea and southwest of Iceland (Fig. 4). The surface salinity is reduced by more than 0.2 psu in these regions, rendering these waters less prone to deep-water formation. In the Labrador Sea, a small northward shift of the convective activity is observed (Fig. 4). There is a 6% decline in the intensity of the overturning cell associated with NADW formation, from 26.2 Sv in CL to 24.6 Sv in OP (Fig. 5). The maximum of the Atlantic meridional stream function at 30 °S, which may be interpreted as the NADW export to the other oceans, drops from 15.8 Sv to 14.9 Sv. In general, the freshwater transport through the Bering Strait leads to a reduced thermohaline circulation in the northern Atlantic.

In the Atlantic, the northward flow at intermediate depths is smaller in OP than in CL, owing to the decline in the thermohaline circulation and the increase of the southward flow through Fram Strait (Fig. 5). In OP, the upwelling of intermediate waters in the North Pacific (not shown) is enhanced and that water feeds the Bering Strait throughflow.

The thermohaline circulation in the Atlantic carries heat northwards, since the NADW transported southwards is colder than the compensating surface and intermediate-depth flow. Consequently, the reduction of the

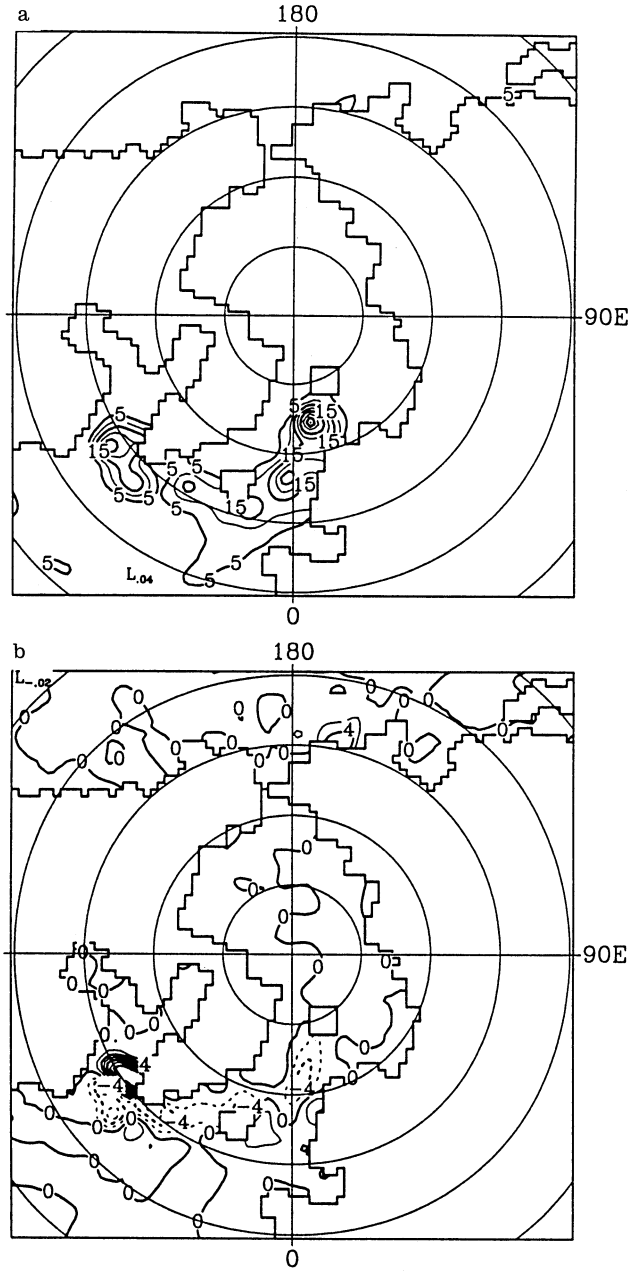

Fig. 4a, b. Energy dissipated by convective adjustment. **a** Experiment OP; contour interval is $5 \times 10^{-3}\,\mathrm{Wm}^{-2}$. **b** OP minus CL; contour interval is $2 \times 10^{-3}\,\mathrm{Wm}^{-2}$

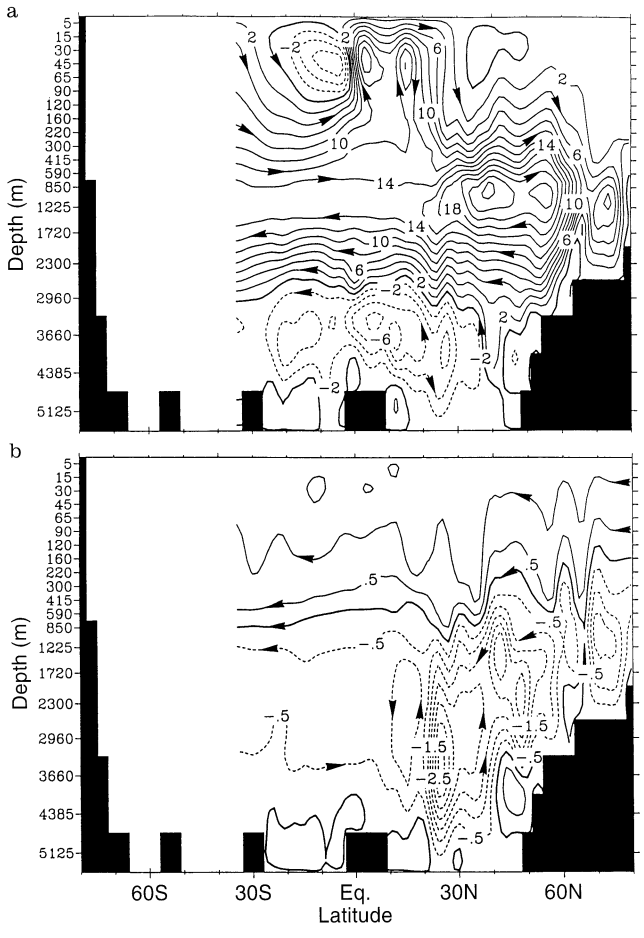

Fig. 5a, b. Annual mean meridional overturning stream function in the Atlantic. **a** Experiment OP; contour interval is 2 Sv. **b** OP minus CL; contour interval is 0.25 Sv. Flow is *clockwise* around *solid contours*

thermohaline circulation when the Bering Strait is open tends to decrease the northward heat transport. For example, the latter is, at 30 °S in the Atlantic, 3.5×10^{14} W in CL and 3.1×10^{14} W in OP. The heat flux crossing the equator is 8.8×10^{14} W in CL and 8.4×10^{14} W in OP. As the heat transported by the ocean is transferred to the atmosphere north of 25 °N, the reduction in the northward heat transport corresponds to a decrease of the heat flux from the ocean to the atmosphere in this region. This decrease amounts to 2 W/m^2 when averaged over the Atlantic north of 25 °N.

Figure 6 displays the difference of the freshwater transport in the ocean between the experiments OP and CL.

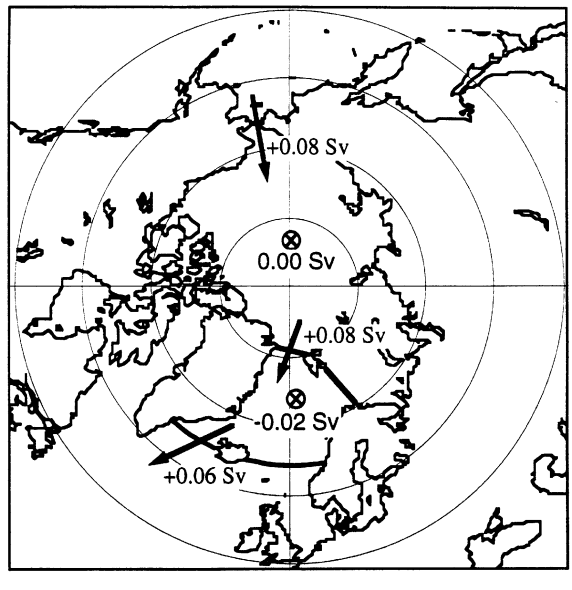

Fig. 6. Difference of freshwater transport in the ocean and of surface freshwater fluxes between OP and CL (OP minus CL)

The inflow through the Bering Strait is of 1.15 Sv, with a salinity of 32.5 psu. Considering a reference salinity of 35 psu (this is close to the salinity in GIN Sea and North Atlantic, the regions of particular interest in this study), this inflow corresponds to a freshwater flux of 0.08 Sv.

The surface freshwater fluxes in the Arctic are identical in the two experiments (0.17 Sv). A small increase in ice production (-0.001 Sv) in OP is compensated by the stronger effect of the surface restoring to Levitus' salinity in this experiment ($+0.01$ Sv). Therefore, the difference of freshwater transport is not affected by surface fluxes in the Arctic. The 0.08 Sv freshwater transport associated with the Bering Strait throughflow is totally transferred to the GIN Sea.

In the GIN Sea, the restoring procedure leads to a freshwater flux smaller by 0.02 Sv when the Bering Strait is open, because of the lower salinity of this region. This flux difference is mainly located along the coast of Greenland where the difference of salinity is the strongest (Fig. 3a). The evaporation decreases by about 0.01 Sv in OP, due to the decrease in sea-surface temperature. Furthermore, as pointed out previously, the ice melting is smaller by 0.01 Sv in the GIN Sea in OP. As a consequence, the surface freshwater flux in the GIN Sea is 0.02 Sv smaller when the Bering Strait is open, which tends to decrease the influence of the freshwater flow through the Bering Strait. This difference is partly due to a modification of the surface forcing (-0.01 Sv: restoring and evaporation) and partly to a freshwater transport in the model caused by the ice advection (-0.01 Sv: decrease of net ice melting). The opening of the Bering Strait thus yields in OP a freshwater transport to the North Atlantic Ocean of 0.06 Sv.

The freshwater budget of the Atlantic between Iceland and 30 °S hardly changes between OP and CL. The simulated net evaporation amounts to 0.4 Sv in the two experiments. The precipitation is held constant in the model and the evaporation decreases by 0.008 Sv in OP compared to CL. The only significant modification in the freshwater budget is the increased ice melting southwest of Iceland in OP ($+0.02$ Sv). As a consequence, in our experiments, the simulated freshwater transport from the Pacific to the North Atlantic (0.06 Sv) accounts for about 10% of the freshwater deficit of the Atlantic (0.4 Sv).

The differences between OP and CL must be interpreted with some caution, because the surface forcing is derived from atmospheric measurements carried out during the present century, i.e., over a period of time during which the Bering Strait is open. Upon closing the Bering Strait, the atmospheric conditions are likely to undergo some modifications, which we have not been able to take into account in our experiments. The best strategy would certainly consist of using a coupled ocean-atmosphere general circulation model. However, such a model is still too expensive to be applied to the present kind of study.

Our numerical experiments reveals that the main effect of the opening of the Bering Strait on the freshwater budget of the GIN Sea is the freshwater flux associated with the throughflow, rather than the mere flow or any indirect effect (see Appendix). However, the type of forcing used here implicitly assumes that the atmospheric feedback is of secondary importance. This assumption limits the validity of our results as the amplification or damping by atmospheric feedback of the perturbation caused by opening/closing the Strait could modify our conclusions. However, it is believed that this sensitivity study has reproduced a first-order effect of the influence of the Bering Strait and described a plausible mechanism to explain its influence.

As discussed above, the opening of the Bering Strait induces a modification of the model freshwater forcing. These changes in the restoring and in the evaporation without any change in the precipitation do not correctly reproduce the behaviour of the atmosphere. The equivalent freshwater fluxes induced by the restoring are of a particularly spurious nature, since they are caused by relaxation towards surface salinities observed in a configuration with the Bering Strait open even when the simulation pertains to a closed Bering Strait case. These differences in freshwater fluxes are not negligible (maximum 0.02 Sv) compared with the freshwater fluxes associated with the flow through the Bering Strait (0.08 Sv). They can affect the response of the model to the opening of the Bering Strait. However, they are at least four times smaller than the freshwater transport induced by the opening of the Bering Strait. We are thus inclined to conclude that the differences in the freshwater forcing do not invalidate our results.

The surface salinity relaxation must be strong enough to prevent a global salinity drift, but must be sufficiently weak so that the impact of the Bering Strait on the World Ocean's circulation is not offset by spurious freshwater fluxes at the air–sea interface. For example, Reason and Power (1994) used a relaxation time scale of 20 days over a 25 m-depth level, which corresponds to a restoring 7.5 times stronger than the one applied in the present study. Applying this restoring, with the same salinity changes in the GIN Sea as in our experiments, would imply a flux associated with the restoring 7.5 times larger than in the case presented here. Therefore, the modification of the restoring flux would have been of the same magnitude as the freshwater flux associated with the Bering Strait throughflow. On the other hand, if the modifications in the freshwater fluxed induced by the restoring were the same as the one obtained in our study, the salinity difference between the experiments with Bering Strait open and closed would have been 7.5 smaller with this strong restoring. It would thus have a very small impact on density and thus on deep-water formation. Unfortunately, Reason and Power (1994) do not show their diagnosed freshwater fluxes. We are thus obliged to make speculations about their results. However, the two extreme cases presented here clearly show that the restoring can pose some problems in their study. These remarks seem to be also valid for the mixed boundary condition case of Reason and Power (1994) in which the two sets of surface freshwater fluxes are deduced from the corresponding restoring cases (i.e., Bering open and closed) using Levitus' (1982) data in both cases. The differences between the freshwater fluxes applied in the two mixed boundary cases (Bering open and closed) are thus the same as between the two restoring cases. Note that the study of the impact of the Bering Strait on the oceanic circulation was not the only goal of the paper of Reason and Power (1994). It is the reason

why they use two different sets of surface fluxes in their two experiments.

5 Conclusions

The impact of the water flow through the Bering Strait on the World Ocean's circulation has been studied with the help of a large-scale, coupled ice–ocean general circulation model. The Bering Strait throughflow induced a transport of freshwater from the North Pacific to the GIN Sea, the transport being almost not affected by the transit in the Arctic. This transport is an important element of the freshwater budget of the Atlantic since it compensates for more than 10% of the freshwater deficit of the Atlantic. As a consequence, on opening the Bering Strait, the surface salinity in the GIN Sea decreases, inducing a 6% decline in the intensity of the NADW overturning cell and of the southward export of NADW. The weakening of the thermohaline circulation leads to a decrease of the northward heat transport in the Atlantic of roughly 5%.

The surface forcing must be considered with caution when interpreting the results, since no atmospheric feedback is allowed in our experiments. The modification of the atmospheric forcing associated with the opening of Bering Strait and the consequences of these changes on the oceanic circulation can not reliably taken into account here. Furthermore, a weak restoring to the present-day surface salinity is applied in the two experiments (Bering open or closed). Nevertheless, the freshwater flux difference induced by the restoring between the experiments with Bering Strait open or closed is much smaller than the flux induced by the flow through the Strait. Thus, it appears that these restoring fluxes are of secondary importance in our simulation. The contrasting results of Reason and Power (1994), compared to the ones presented here, may be due to the changes in surface forcing between their experiments with Bering Strait open and closed offsetting the effect of the Bering Strait. It is worth stressing that the restoring tends to limit the influence of the flow through the Bering Strait in our experiments.

Our results are qualitatively in agreement with those obtained by Shaffer and Bendtsen (1994) with a box model. In their study, however, a much stronger response to the Bering Strait throughflow was found. For example, a transport of 1.1. Sv through the Bering Strait led to a complete suppression of deep-water formation in the North Atlantic. An additional numerical experiments has been conducted with our model in which the flow through the Bering Strait has been enhanced to 2.1 Sv (the parameter α intervening in the parametrization of the throughflow was taken equal to unity; see Sect. 3). This modification induces a reduction of the thermohaline circulation of 11% compared to the case when the Bering Strait transport was 1.15 Sv (weakening of 17% compared to the case with Bering Strait closed), but the thermohaline circulation does not collapse in the Atlantic. However, with the type of forcing used (restoring), the results are forced to remain close to present-day values. As a consequence, the question as to whether a collapse of the thermohaline circulation in the Atlantic can be caused by an increased flow through Bering Strait can hardly be answered with this type of forcing.

In some ocean models, the flow through the Bering Strait is not taken into account. The present work seems to validate this approach as the influence of the Bering Strait on the global ocean circulation seems to be well within the order of magnitude of the uncertainties of current ocean models. Nevertheless, the opening of Bering Strait has notable consequences for the freshwater budget of the Atlantic. Since this budget appears to be important for the stability of the thermohaline circulation, it might have an influence on the response of the climatic system to a perturbation. Furthermore, the cost of representing the Bering Strait throughflow in an OGCM is so small that it should probably be done.

Acknowledgements. We want to thank Dr. J. Overland for valuable discussions about the parametrization of the flow through the Bering Strait. The comments of Dr. S. Rahmstorf and an anonymous reviewer were very much appreciated. Professor E. Wolanski, Dr. M.A. Morales Maqueda, Ph Tulkens and B. Tartinville helped to improve the clarity of the manuscript. We also want to thank the different data centers which provided us with atmospheric data (see references in the text), particularly the Data Support Section of the Scientific Computing Division of the National Center for Atmospheric Research. For this work, J.M. Campin was sponsored by an European Community grant (contract CEE S/EVSV/92310). T. Fichefet and E. Deleersnijder are sponsored by the National Fund for Scientific Research (Belgium). This work was done within the scope of the Impulse Programme "Global Change" (Belgian State, Prime Minister's Services, Federal Office for Scientific, Technical and Cultural Affairs (OSTC), Contract GC/10/013), the Convention d'Action de Researches Concertées 092/97-154 with the Communauté Française de Belgique and the Programme National d'Impulsion en Technologie de l'Information (Belgian State, Prime Minister's Services, Federal Office for Scientific, Technical and Cultural Affairs (OSTC), Contract IT/SC/20), the European Environment and Climate Programme (Contract EV5V-CT92-0123), and a study contract with Digital Europe (External Research Agreement, Contract BE-011) which allowed us to use a DEC 2100 workstation. All these supports are gratefully acknowledged.

Appendix

The salinity budget of the GIN Sea

In our discussion, the GIN Sea covers the area located between Greenland and Norway, bounded to the south by a latitudinal circle at 65 °N and to the north by a broken line from northern greenland to Cape North in Norway, passing through Spitzbergen (see the heavy line in Figs. A1 and A2).

The salinity changes in this region seems to be very important for the response of our model to the opening of the Bering Strait. As a consequence, a salinity budget of the GIN Sea is used to gain a more precise idea of the role of the various freshwater and salt fluxes on the evolution of the salinity in this region. In the simple method presented here, the GIN Sea is represented by a perfectly mixed "box" with a salinity $\overline{S}$. The "box" is forced at its boundaries by the fluxes obtained in our simulations.

Firstly, the numerical experiment in which the Bering Strait is closed is considered (experiment CL; Fig. A1). The inflow from the Atlantic amounts to 18.9 Sv, with a

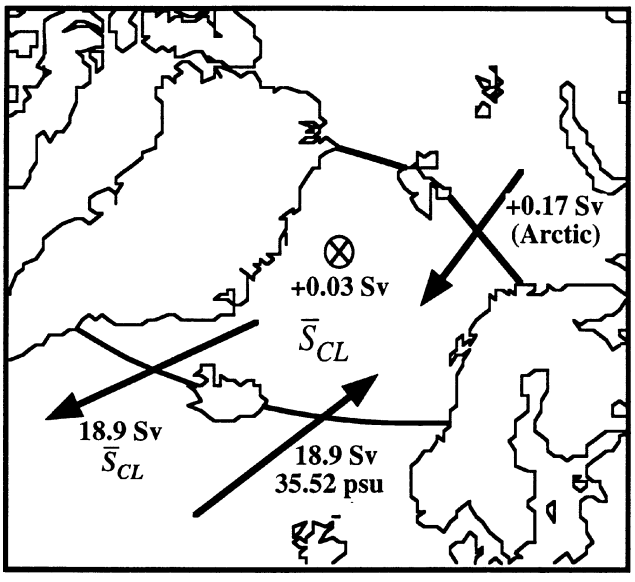

Fig. A1. Salt and freshwater budget of the GIN Sea when the Bering Strait is closed (experiment CL). See text for details

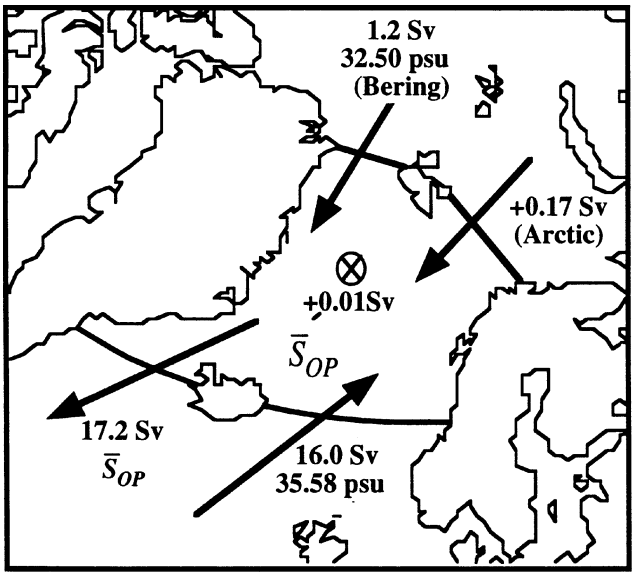

Fig. A2. Same as A1, except that Bering Strait open (experiment OP)

salinity of 35.52 psu. This is the major inflow to the GIN Sea. For simplicity, the exchanges with the Arctic are only described as a net freshwater flux (+0.17 Sv) to GIN Sea. The surface freshwater flux is 0.03 Sv in experiment CL. As we assume that the GIN Sea is perfectly mixed, the salinity of the 18.9 Sv outflow through Denmark Strait is equal to $\bar{S}$ (called $\bar{S}_{CL}$ in experiment CL). The salt and freshwater balance of the GIN Sea leads to value of $\bar{S}_{CL}$:

$$\bar{S}_{CL} = \frac{18.9 \times 35.52 - (0.17 + 0.03) \times 35}{18.9}$$

considering a reference salinity of 35. Note that the results are not sensitive to the choice of this reference.

When the Bering Strait is open (experiment OP), the Arctic receives a net surface freshwater flux of 0.17 Sv and roughly 1.2 Sv flows through the Bering Strait with a salinity of 32.5 psu. To close the budget of the Arctic, those mass and salt fluxes must be balanced by the exchanges with the GIN Sea. As a consequence, the transport from the Arctic to the GIN Sea can be described by two terms. The first one is equivalent to a 0.17 Sv freshwater flux to the GIN Sea (as in CL) and the second one is represented by a flow of 1.2 Sv of water with a salinity of 32.5 psu.

In OP, the surface freshwater flux to the GIN Sea is of 0.01 Sv; the inflow from the Atlantic carries 160 Sv at an averaged salinity of 35.58 psu; the outflow transports 17.2 Sv southward to verify the mass balance in the GIN Sea. The salinity $\bar{S}_{OP}$ can be obtained as above:

$$\bar{S}_{OP} = \frac{16.0 \times 35.58 + 1.2 \times 32.50 - (0.17 + 0.01) \times 35}{17.2}$$

The salinity difference between the two experiments can be seen as the sum of four terms:

$$\begin{aligned}\bar{S}_{OP} - \bar{S}_{CL} = & + \frac{1.2}{17.2}(32.50 - 35.58) - \left(\frac{0.01}{17.2} - \frac{0.03}{18.9}\right) \times 35 \\ & - \left(\frac{0.17}{17.2} - \frac{0.17}{18.9}\right) \times 35 + (35.58 - 35.52) \\ = & -0.21 + 0.04 - 0.03 + 0.06 \\ = & -0.14\end{aligned}$$

The first term is associated with the net mass flow from the Arctic, consequence of the opening of the Bering Strait (−0.21 psu). The second one is caused by the modification of the surface fluxes (+0.04 psu). The third term comes from the decrease of the inflow from the Atlantic, which increases the "dilution" of this water by the freshwater from the Arctic and thus reduces the salinity (−0.03 psu). The last one is due to the difference of the salinity of the Atlantic water transported to the GIN Sea between the two experiments (+0.06 psu).

This simple method shows that the decrease of the salinity in the GIN Sea when the Bering Strait is open is mainly a consequence of the freshwater transport induced by the opening of the Bering Strait. None of the other terms invoked is negligible, but they seem to have a smaller impact.

References

Baumgartner A, Reichel E (1975) The world water balance. Elsevier, Amsterdam

Berliand ME, Strokina TG (1980) Global distribution of the total amount of clouds (in Russian), Hydrometeorological Publishing House, Leningrad

Broecker WS (1991) The great ocean conveyor. Oceanography 4:79–89

Broecker WS, Peng TH, Jouzel J, Russel G (1990) The magnitude of global fresh-water transports of importance to ocean circulation. Clim Dyn 4:73–79

Bryan K (1969) A numerical method for the study of the circulation of the world ocean. J Comput Phys 4:347–376

Coachman LK, Aagaard K (1988) Transports through Bering Strait: annual and interannual variability. J Geophys Res 93: 15535–15539

Coward AC, Killworth PD, Blundell JR (1994) Tests of a two-grid world ocean model. J Geophys Res 99: 22725–22735

Crutcher HL, Meserve JM (1970) Selected level heights, temperatures and dew points for the Northern Hemisphere. NAVAIR 50-1C-52 Revised, Naval Weather Service, Washington DC

Deleersnijder E (1994) An analysis of the vertical velocity field computed by a three-dimensional model in the region of the Bering Strait. Tellus 46A: 134–148

Deleersnijder E, Campin JM (1995) On the computation of the barotropic mode of a free-surface world ocean model. Ann Geophys 13: 675–688

Deleersnijder E, van Ypersele JP, Campin JM (1993) An orthogonal curvilinear coordinate system for a World Ocean model. Ocean Modell 100: 7–10 (+figures)

Eby M, Holloway G (1994) Grid transformation for incorporating the Arctic in a global ocean model. Clim Dyn 10: 241–247

Fichefet T, Gaspar P (1988) A model study of upper ocean–sea ice interactions. J Phys Oceanogr 18: 181–195

Gloersen P, Campbell WJ, Cavalieri DJ, Parkinson CL, Zwally HJ (1992) Arctic and Antarctic sea ice, 1978–1987: satellite passive-microwave observations and analysis. NASA SP-511, Washington DC

Häkkinen S, Mellor GL (1990) One hundered years of Arctic ice cover variations as simulated by a one-dimensional, ice–ocean model. J Geophys Res 95: 15959–15969

Hibler WD (1979) A dynamic thermodynamic sea ice model. J Phys Oceanogr 9: 815–846

Hibler WD (1986) Ice dynamics. In: Untersteiner N (ed) The geophysics of sea ice. NATO ASI Series, vol 146. Plenum Press, New York, pp 577–640

Jaeger L (1976) Monatskarten des Niederschlags für die ganze Erde (in German). Ber Dtsch Wetterdienstes 18, No 139

Ledley TS (1985) Sensitivity of a thermodynamic sea ice model with leads to time step size. J Geophys Res 90: 2251–2260

Levitus S (1982) Climatological atlas of the World Ocean. Nat Ocean Atmos Adm Prof Pap 13, US Government Printing Office, Washington DC

Muench RD, Schumacher JD, Salo SA (1988) Winter currents and hydrographic conditions on the northern central Bering Sea Shelf. J Geophys Res 93: 516–526

Nihoul JCJ, Adam P, Brasseur P, Deleersnijder E, Djenidi S (1993) Three-dimensional general circulation model of the Northern Bering Sea's summer ecohydrodynamics. Cont Shelf Res 13: 509–542

Oberhuber JM (1988) An atlas based on the COADS data set: the budgets of heat, buoyancy and turbulent kinetic energy at the surface of the global ocean. Max-Planck-Institut für Meteorologie, Rep 15, Hambourg, Germany

Overland JE, Roach AT (1987) Northward flow in the Bering and Chukchi Seas. J Geophys Res 92: 7097–7105

Pacanowski RC, Philander SGH (1981) Parameterization of vertical mixing in numerical models of tropical oceans. J Phys Oceanogr 11: 1443–1451

Pease CH, Salo SA (1987) Sea ice drift near Bering Strait during 1982. J Geophys Res 92: 7107–7126

Rahmstorf S (1995) Climate drift in an ocean model coupled to a simple, perfectly matched atmosphere. Clim Dyn 11: 447–458

Reason CJC, Power SB (1994) The influence of the Bering Strait on the circulation in a coarse resolution global ocean model. Clim Dyn 9: 363–369

Roach AT, Aagaard K, Pease CH, Salo SA, Weingartner T, Pavlov V, Kulakov M (1995) Direct measurements of transport and water properties through the Bering Strait. J Geophys Res 100: 18443–18457

Simonsen K, Haugan PM (1996) Heat budgets of the Arctic Mediterranean and sea surface heat flux parametrizations for the Nordic Seas. J Geophys Res 101: 6353–6376

Shaffer G, Bendtsen J (1994) Role of the Bering Strait in controlling North Atlantic ocean circulation and climate. Nature 367: 354–357

Stigebrandt A (1984) The North Pacific: a global-scale estuary. J Phys Oceanogr 14: 464–470

Taljaard JJ, van Loon H, Crutcher HL, Jenne RL (1969) Climate of the upper air, Part I. Southern Hemisphere, vol. 1, temperatures, dew points, and heights at selected pressure levels. NAVAIR 50-1C-55, US. Naval Weather Service, Washington D.C., USA

Toulany B, Garrett C (1984) Geostropic control of luctuating barotropic flow through straits. J Phys Oceanogr 14: 464–470

Trenberth KE, Olson JG, Large WG (1989) A global ocean wind stress climatology based on ECMWF analyses. National Center for Atmos Res, NCAR/TN-338 + STR, Boulder, Colorado

Walsh JJ, McRoy CP, Coachman LK, Goering JJ, Nihoul JCJ, Whitledge TE, Blackburn TH, Parker PL, Wirick CD, Shuert PG, Grebmeier JM, Springer AM, Tripp RB, Hansell DA, Djenidi S, Deleersnijder E, Henriksen K, Lund BA, Andersen F, Müller-Karger FE, Dean K (1989) Carbon and nitrogen cycling within the Bering/Chukchi Seas: source regions for organic matter effecting AOU demands of the Arctic Ocean. Prog Oceanogr 22: 277–359

Wijffels SE, Schmitt RW, Bryden HL, Stigebrandt A (1992) Transport of freshwater by the oceans. J Phys Oceanogr 22: 155–162